Thin-Walled Graphitic Nanocages As a Unique Platform for Amperometric Glucose Biosensor

Chun Xian Guo,[†,‡] Zhao Min Sheng,[†,‡] Yi Qiang Shen,[§] Zhi Li Dong,[§] and Chang Ming Li*[,‡]

School of Chemical and Biomedical Engineering & Center for Advanced Bionanosystems, Nanyang Technological University, 70 Nanyang Drive, Singapore 637457, School of Material Science and Engineering, Nanyang Technological University, 70 Nanyang Avenue, Singapore 639798

ABSTRACT A thin-walled graphitic nanocages material with well-developed graphitic structure, large specific surface area and pronounced mesoporosity was synthesized and used to construct a sensing interface for an amperometric glucose biosensor, showing a high and reproducible sensitivity of 13.3 μA mM^{-1} cm^{-2}, linear dynamic range of 0.02−6.2 mM, and fast response time of 5 s. It was successfully used to accurately detect glucose in human serum with effective discrimination to common interference species such as dopamine, ascorbic acid, acetaminophen, and uric acid.

KEYWORDS: graphitic nanocages • mesoporous carbons • glucose biosensor • electron transfer

The development of enzymatic biosensors has become an active research area as it plays an important role in the clinical and industrial applications (1−4). A major goal in enzymatic biosensors is to develop novel types of biosensors with high sensitivity, fast response, good selectivity, and long-term stability for various applications (5−7). Different approaches have been developed, among which the use of functional nanomaterials has attracted great attention because they can efficiently facilitate electron transfer between enzyme and electrode, while allowing the detection at low potentials (8−10). Among various kinds of functional nanomaterials, mesoporous carbons have attracted increasing interest because of their advantages of suitable mesoporosity, high specific surface area and large pore volume (11). Different kinds of mesoporous carbons such as bicontinuous gyroidal carbon for myoglobin (12), whiskerlike carbon for hemoglobin (13), ordered mesoporous carbons for glucose oxidase (GOD) (14), and porous carbon aerogel for multicopper oxidases (15), have been fabricated and used to construct enzymatic biosensors. However, the currently reported mesoporous carbons are always poorly graphitized, resulting in relative poor conductivity (16, 17). Good conductivity of an electrode material is very essential to achieve a high-performance biosensor (18, 19). Therefore, mesoporous carbons with well-developed graphitic structure in biosensing applications are highly needed.

Herein, we present an enzymatic glucose biosensor based on thin-walled graphitic nanocages with well-developed graphitic structure and distinguished hollow interiors. The prepared glucose biosensor exhibits a high and reproducible sensitivity, broad linear dynamic range, and fast response. It is successfully used to accurately detect glucose in human serum with effective discrimination to common interference species such as dopamine, ascorbic acid, acetaminophen, and uric acid.

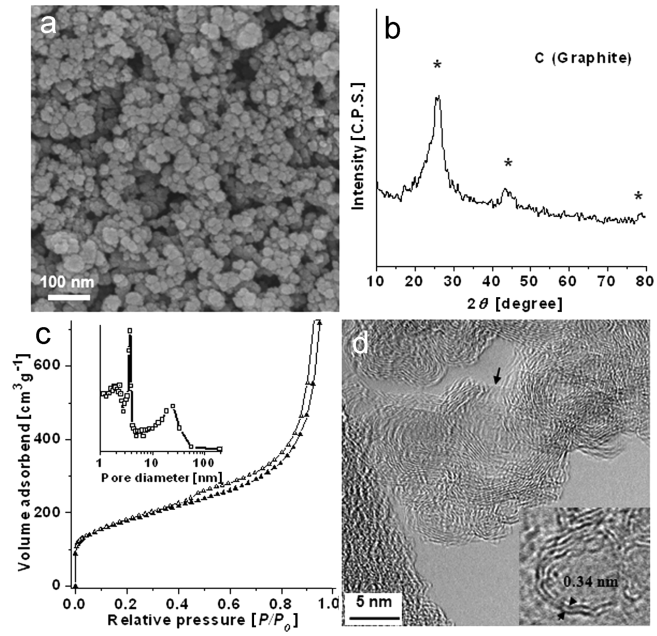

FIGURE 1. (a) SEM image, (b) XRD, (c) nitrogen adsorption/desorption isotherms, and (d) TEM image of graphitic nanocages. Inset of c is the pore size distribution. Inset of d is the HRTEM image showing the graphitic layer space of 0.34 nm.

The structure of prepared graphitic nanocages was characterized. SEM image (Figure 1a) illustrates that the nanocages have particlelike structure with quite uniform size. The XRD pattern in Figure 1b shows three peaks at around 26, 44, and 78°, which can be assigned to the reflections of graphitic planes (002), (101), and (110) respectively (11),

* Corresponding author. Tel.: +65 67904485. Fax: +65 67911761. E-mail: ecmli@ntu.edu.sg.

Received for review May 30, 2010 and accepted August 16, 2010

† These authors made an equal contribution to this work.

‡ School of Chemical and Biomedical Engineering & Center for Advanced Bionanosystems, Nanyang Technological University.

§ School of Material Science and Engineering, Nanyang Technological University.

DOI: 10.1021/am100472j

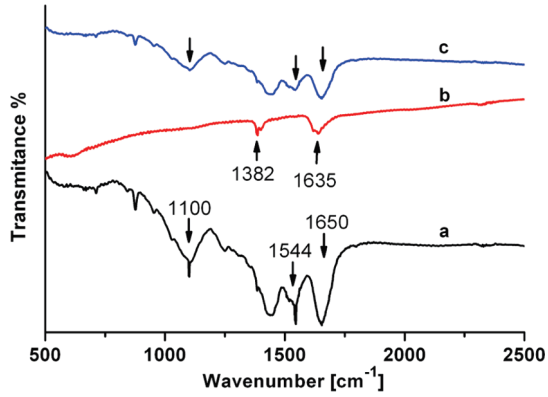

FIGURE 2. FTIR spectra of (a) GOD, (b) graphitic nanocages, and (c) GOD/graphitic nanocages.

suggesting the nanocages have well-developed graphitic structure. Their specific surface area calculated from the nitrogen adsorption/desorption isotherms (Figure 1c), is as high as 613 $m^2 g^{-1}$, much larger than other graphitic carbons such as SWNTs and MWNTs (20). According to BJH method, the pores are mainly distributed from 3 to 20 nm (inset of Figure 1c). The well-developed graphitic structure is further confirmed by TEM (Figure 1d). TEM image displays that the nanocages consist of hollow interiors and their walls are made up of several graphitic layers with a distance around 0.34 nm (inset of Figure 1d). Some defects induced by HNO_3 treatment are also observed (arrow in Figure 1d) on walls of nanocages, making them suitable hosting matrix for enzyme immobilization. Considering the well-developed graphitic structure, larger specific surface area, and pronounced mesopore size distributions, the nanocages can be a good candidate to immobilize enzyme for sensitive biosensing.

The conformational change of the enzyme GOD immobilized on graphitic nanocages was examined by IR spectroscopy, an efficient tool to study the bioactivity related secondary structure of proteins (5). Two obvious IR absorption bands centered at 1650 and 1544 cm^{-1} are observed for GOD itself (Figure 2a), ascribing to the typical amide I and II adsorption band, respectively (19). Another band around 1100 cm^{-1} is also seen, corresponding to the stretching vibration of C−O of GOD (19). The graphitic nanocages exhibit bands at 1382 and 1635 cm^{-1} (Figure 2b), which correspond to the C═O stretching vibrations from ketones or carboxyl groups (11). For GOD immobilized on graphitic nanocages (Figure 2c), it is clear that both amide I and II bands have almost no change. Moreover, the stretching vibration band around 1100 cm^{-1} is still here. Thus, the FTIR spectra suggest that GOD can hold its native structure on graphitic nanocages. This is particularly critical to make GOD functionable for enzymatic activity.

The electrochemical property of the GOD/graphitic nanocages modified glassy carbon electrode (GCE) was studied. From curve 3 in Figure 3a, GOD/graphitic nanocages modified GCE exhibits a pair of well-defined redox peaks at −0.434 and −0.391 V, consistent with reported values for $FAD/FADH_2$, the active sites of GOD at neutral pH (14). By contrast, no obvious redox peaks are observed on GOD (or

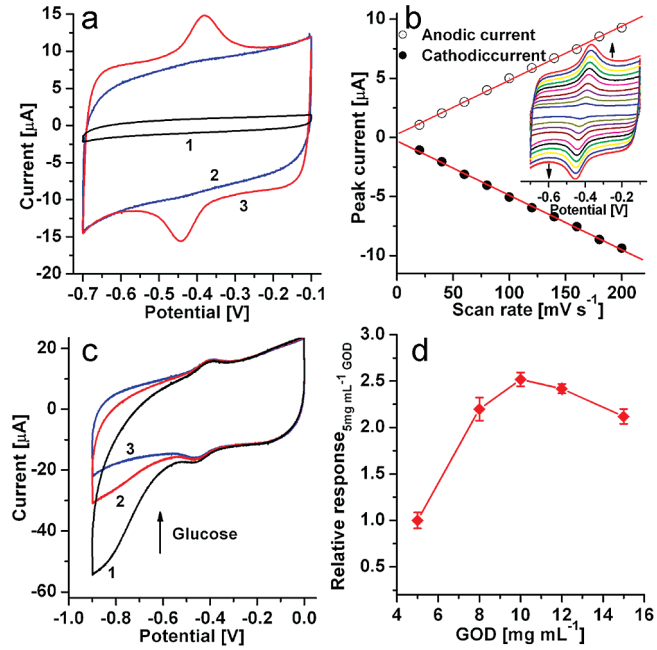

FIGURE 3. (a) Cyclic voltammograms (CVs) of different materials modified glassy carbon electrodes (GCEs) in 0.1 M N_2-saturated PBS (pH 7.0) at 100 mV s^{-1}. (1) GOD, (2) graphitic nanocages, and (3) GOD/graphitic nanocages. (b) Plots of peak current versus scan rate for GOD/graphitic nanocages modified GCE. (c) CVs of GOD/graphitic nanocages modified GCE in 0.1 M air-saturated PBS (pH 7.0) with different glucose concentrations: (1) 0, (2) 5, and (3) 10 mM. (d) Plot of relative response of GOD/graphitic nanocage modified GCE in 0.1 M air-saturated PBS (pH 7.0) containing 5 mM glucose versus the GOD immobilization concentration.

graphitic nanocage) modified GCE alone. Interestingly, graphitic nanocage modified GCE exhibits a well-squared CV curve, which might be caused by their large double layer capacitance, resulting from the highly porous structure. The property of redox reaction process of GOD immobilized on graphitic nanocages was studied by varying the scan rate. It is found from Figure 3b that the redox peak currents increase linearly with scan rates from 20 to 200 mV s^{-1}, indicating the redox reaction is a surface-controlled electrochemical process (5) and the redox signals really come from GOD immobilized on graphitic nanocages. Calculated from Laviron equation (21), the electron transfer rate constant (k_s) of GOD on graphitic nanocages is 5.84 s^{-1}, much higher than that of GOD on ordered mesoporous carbon (3.92 s^{-1}) (14), MWNTs (1.53 s^{-1}) (22), and SWNTs (0.3 s^{-1}) (23). Apparently, the graphitic nanocages can more efficiently facilitate electron transfer between active sites of GOD with electrode. The electrocatalytic behavior of GOD/graphitic nanocages modified GCE toward glucose was examined. When glucose with different concentrations is added, the reduction peak current gradually decreases (Figure 3c), whereas no response is observed for graphitic nanocage modified GCE. These results demonstrate GOD immobilized on graphitic nanocages retains its catalytic activity toward glucose. Similar observations have also been reported on other GOD-immobilized electrodes and this phenomenon is always used to detect glucose in glucose biosensors (5, 14, 22). The glucose sensing mechanism is a GOD direct electron transfer process with competitive glucose oxidation and oxygen

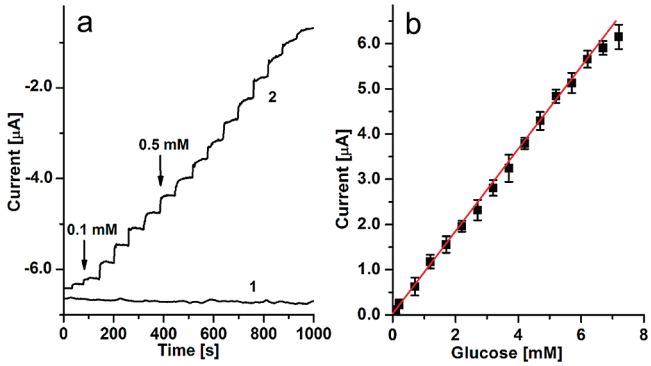

FIGURE 4. (a) Amperometric responses of (1) graphitic nanocage modified GCE and (2) GOD/graphitic nanocage modified GCE to successive additions of glucose in stirred 0.1 M air-saturated PBS (pH 7.0) at −0.5 V. (b) The calibration curve from curve 2 of panel a.

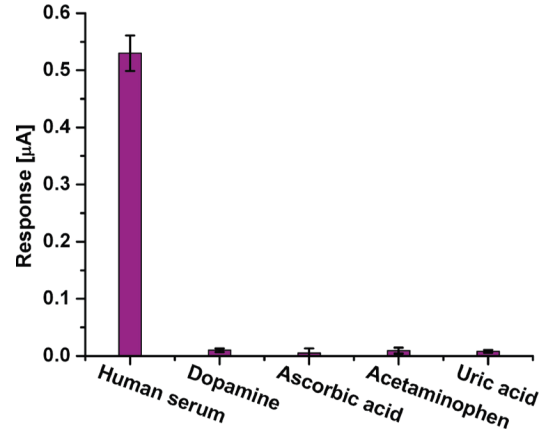

FIGURE 5. Comparison of the response of GOD/graphitic nanocages modified GCEs to human serum (100 μL, male serum), dopamine (0.1 mM), ascorbic acid (0.1 mM), acetaminophen (0.1 mM), and uric acid (0.1 mM) in 900 μL of stirred 0.1 M air-saturated PBS (pH 7.0) at −0.5 V.

reduction, which has been systematically studied recently by us (24). By comparing the GOD catalytic behavior in air-saturated and in nitrogen-saturated glucose solution, it is found that the response in air-saturated glucose solution is larger than that in nitrogen-saturated glucose solution (24), and thus the presence of oxygen has a positive effect on sensitivity of glucose detection. The effect of GOD immobilization concentration on the catalytic performance toward glucose oxidation was investigated. As shown in Figure 3d, the highest response of the electrode is obtained at GOD concentration around 10 mg mL^{-1}.

The performance of the biosensor toward glucose is evaluated by amperometric response to successive additions of glucose at −0.5 V. As shown in Figure 4a (curve 2), immediately after the addition of glucose, the current changes and reaches a steady state within 5 s. The calibration plot based on the change of the steady-state current is shown in Figure 4b. The linear response range is from 0.02 to 6.2 mM with a detection limit of 8 μM for a signal-to-noise ratio of 3. The sensitivity of the sensor determined from the slope is 13.3 μA mM^{-1} cm^{-2}. The analytical performance of the biosensor is compared with some other glucose biosensors and the results are summarized in Table S1 in the Supporting Information. Control experiment was also carried out by successive additions of glucose to a graphitic nanocage modified GCE at −0.5 V (curve 1 in Figure 4a), which shows negligible response.

The electrode was further used to detect glucose in human serum (glucose concentration of 5.85 mM, provided in the product information sheet). Figure 5 shows a typical response on injection of 100 μL of the serum into 900 μL of PBS, resulting in 0.53 μA response. Calculated from the response (0.53 μA) and sensitivity (13.3 μA mM^{-1} cm^{-2}) of the biosensor, glucose concentration in the serum is 5.88 mM, which is almost the same with the value of 5.85 mM provided by the manufacturer, suggesting the accurate measurement of the biosensor. Nevertheless, for precise measurement of glucose level in blood of patient with diabetics, dilution of blood sample is still needed. The interference from common interference species such as dopamine, ascorbic acid, acetaminophen and uric acid was also investigated by using their relevant physiological levels (0.1 mM). Injections of these interferences show negligible responses (Figure 5). As a biosensor application, the stability is also critical. When the electrodes were tested by continuous amperometric measurements for 3 h measured at interval of 5 days, and stored at 4 °C when not in use, they could retain 95% of the original response over 4 weeks, demonstrating the remarkable stability. The results of 10 successive measurements show a relative standard deviation of 4.1%. The relative standard deviation of the current responses over 8 sensors prepared with the same procedure did not exceed 6.8%.

In summary, a thin-walled graphitic nanocages material was synthesized and used to fabricate an amperometric glucose biosensor. The unique physicochemical properties of the graphitic nanocages including well-developed graphitic structure, high specific surface area, and pronounced mesoporosity make the biosensor with a high and reproducible sensitivity of 13.3 μA mM^{-1} cm^{-2}, broad linear dynamic range of 0.02−6.2 mM, and accurate measurement of glucose in human serum with effective discrimination from common interference species. The work opens a way to utilize graphitic nanocages as a new promising platform for enzymatic biosensors in practical clinical applications.

Acknowledgment. We acknowledge the financial support from the Center for Advanced Bionanosystems, Nanyang Technological University.

Supporting Information Available: Description of experimental details (PDF). This material is available free of charge via the Internet at http://pubs.acs.org.

REFERENCES AND NOTES

(1) Leger, C.; Bertrand, P. *Chem. Rev.* **2008**, *108*, 2379–2438.
(2) Dong, H.; Cao, X.; Li, C. M. *ACS Appl. Mater. Interfaces* **2009**, *1*, 1599–1606.
(3) Fang, B.; Gu, A.; Wang, G.; Wang, W.; Feng, Y.; Zhang, C.; Zhang, X. *ACS Appl. Mater. Interfaces* **2009**, *1*, 2829–2834.
(4) Yan, J.; Pedrosa, V. A.; Simonian, A. L.; Revzin, A. *ACS Appl. Mater. Interfaces* **2010**, *2*, 748–755.
(5) Bao, S. J.; Li, C. M.; Zang, J. F.; Cui, X. Q.; Qiao, Y.; Guo, J. *Adv. Funct. Mater.* **2008**, *18*, 591–599.
(6) Guo, C. X.; Hu, F. P.; Li, C. M.; Shen, P. K. *Biosens. Bioelectron.* **2008**, *24*, 819–824.

(7) Dey, R. S.; Gupta, S.; Paira, R.; Raj, C. R. *ACS Appl. Mater. Interfaces* **2010**, *2*, 1355–1360.
(8) Ahmed, M.; Deng, Z.; Narain, R. *ACS Appl. Mater. Interfaces* **2009**, *1*, 1980–1987.
(9) Flavel, B. S.; Gross, A. J.; Garrett, D. J.; Nock, V.; Downard, A. J. *ACS Appl. Mater. Interfaces* **2010**, *2*, 1184–1190.
(10) Guo, C. X.; Hu, F. P.; Lou, X. W.; Li, C. M. *J. Power Sources* **2010**, *195*, 4090–4097.
(11) Liang, C. D.; Li, Z. J.; Dai, S. *Angew. Chem., Int. Ed.* **2008**, *47*, 3696–3717.
(12) You, C. P.; Yan, X. W.; Kong, J. L.; Zhao, D. Y.; Liu, B. H. *Electrochem. Commun.* **2008**, *10*, 1864–1867.
(13) Feng, J. J.; Xu, J. J.; Chen, H. Y. *Biosens. Bioelectron.* **2007**, *22*, 1618–1624.
(14) You, C. P.; Xu, X.; Tian, B. Z.; Kong, J. L.; Zhao, D. Y.; Liu, B. H. *Talanta* **2009**, *78*, 705–710.
(15) Tsujimura, S.; Kamitaka, Y.; Kano, K. *Fuel Cells* **2007**, *7*, 463–469.
(16) Sheng, Z. M.; Wang, J. N. *Adv. Mater.* **2008**, *20*, 1071–1075.
(17) Wang, J. N.; Zhang, L.; Niu, J. J.; Yu, F.; Sheng, Z. M.; Zhao, Y. Z.; Chang, H.; Pak, C. *Chem. Mater.* **2007**, *19*, 453–459.
(18) Liu, J. P.; Guo, C. X.; Li, C. M.; Li, Y. Y.; Chi, Q. B.; Huang, X. T.; Liao, L.; Yu, T. *Electrochem. Commun.* **2009**, *11*, 202–205.
(19) Sun, W.; Guo, C. X.; Zhu, Z. H.; Li, C. M. *Electrochem. Commun.* **2009**, *11*, 2105–2108.
(20) Tasis, D.; Tagmatarchis, N.; Bianco, A.; Prato, M. *Chem. Rev.* **2006**, *106*, 1105–1136.
(21) Laviron, E. *J. Electroanal. Chem.* **1979**, *100*, 263–270.
(22) Cai, C. X.; Chen, J. *Anal. Biochem.* **2004**, *332*, 75–83.
(23) Liu, J. Q.; Chou, A.; Rahmat, W.; Paddon-Row, M. N.; Gooding, J. J. *Electroanal.* **2005**, *17*, 38–46.
(24) Guo, C. X.; Li, C. M. *Phys. Chem. Chem. Phys.* **2010**; DOI: 10.1039/C0CP00378F.

AM100472J